Int. J. Solids Structures Vol. 17, No. 11, pp. 1021–1035, 1981
Printed in Great Britain.

0020-7683/81/111021-15$02.00/0
Pergamon Press Ltd.

MAGNETICALLY INDUCED CYLINDRICAL STRESS WAVES IN A THERMOELASTIC CONDUCTOR†

C. T. CHIAN‡
Jet Propulsion Laboratory, Pasadena, CA 91103, U.S.A.

and

F. C. MOON
Department of Theoretical and Applied Mechanics, Cornell University, Ithaca, NY 14853, U.S.A.

(*Received* 5 *July* 1979; *in revised form* 20 *February* 1981)

Abstract—The problem of stress wave generation in a linear thermoelastic solid by a pulsed magnetic field is investigated both analytically and experimentally for a cylindrically symmetric conducting solid. A dynamic response analysis is developed to correlate magnetic, thermal, and stress fields in the solid with the time history of the electric current. In the experiment, a transient magnetic field was applied normal to a large conducting plate with a circular hole. Initially the field was confined to the interior of the circular hole. The field was generated by discharging a large capacitor bank through a solenoidal coil. The plane-stress cylindrical stress waves are 1-D in nature. The relative effects of the magnetic body force and thermoelastic stresses, both generated by the electromagnetic field, are assessed.

INTRODUCTION

The determination of forces, stresses and heat in a conductor when carrying electric current in a magnetic field form a subject of considerable importance in electric power engineering.

For example in magnetic forming, a transient magnetic field in a coil induces eddy currents in an adjacent workpiece thereby generating body forces which deform the solid. In laser machining, high powered electromagnetic radiation is focused on the solid, producing high thermal gradients in the solid, which in turn generate thermoelastic waves that propagate through the material. In modelling the magnetic forming process, the thermoelastic stresses are usually neglected[1], while in the laser machining process only thermoelastic effects and ablative effects are studied[2]. The simultaneous action of these effects is usually not studied.

Moon and Chattopadhay[3] studied the magnetic generation of one-dimensional waves in nonferromagnetic conductors. They were concerned with stress waves in a half-space generated by an applied jump in tangential magnetic field at the boundary. They predicted that two waves are generated by the magnetic field: one is a pressure wave and the other is a thermoelastic wave. The pressure wave is produced by the magnetic body forces, while the thermoelastic wave is produced by the eddy current Joule heating in the plate. They also conducted experiments; however no evidence was observed of the thermal stress pulse.

Inertia effects in a transient thermoelastic problem for a half-space have been investigated by a number of authors. Danilovskaya[4], using uncoupled thermoelasticity and Boley and Tolins[5] using the coupled theory found that a jump in temperature on the surface of a half space will produce a stress wave which will propagate into the solid at the longitudinal wave speed. In [3] Moon and Chattopadhyay found that a step rise in magnetic field at the surface of a half space would produce an instantaneous jump in temperature at the surface and consequently a thermoelastic wave with stress reversal of the type found in [4, 5]. The stress in the thermoelastic wave was found to be five times the magnitude of the stress produced by magnetic body forces.

However Sternberg and Chakravorty[6], treated the half space with a *finite rise time* for the temperature on the surface. A ramp-type temperature field was considered to be applied at the

†This work was supported by a grant from the National Science Foundation (Grant No. ENG 76-23527) to Cornell University.

‡Formerly, Graduate Student, Department of Theoretical and Applied Mechanics, Cornell University, Ithaca, NY 14853, U.S.A.

surface boundary. It was found that if the maximum surface temperature is reached in as short a period as 10^{-12} sec (for steel), the maximum stress attains a value of only about 14% of that when the surface temperature is suddenly changed. They concluded that the increment of stresses due to sudden heating is very small and for practical purposes it is sufficient to assume the quasi-static state.

In this paper, the work of Moon and Chattopadhyay[3] has been extended to investigate magnetically induced stresses and waves in a cylindrical thermoelastic conductor. The material considered here is of finite conductivity, with no magnetic or electric polarization. A dynamic analysis is developed to correlate magnetic, thermal and stress fields in the solid with the time history of the electric currents. The purpose of this study is to assess the relative effects of the magnetic body force and thermoelastic stresses produced by Joule heating.

In the experiments, a transient magnetic field was applied normal to a large conducting plate with a circular hole and the field initially confined to the interior of the hole. The field was generated by discharging a large capacitor bank through a solenoidal coil. The current pulse had a *finite* rise time and the Joule heating produced by eddy currents was confined in some finite boundary layer adjacent to the circular hole.

Since the thermal diffusion time is much greater than the stress wave travel time, the temperature remains effectively steady within the layer, while the stress wave propagates outward from the layer. The problem is solved in two different regions: within the thermal boundary layer, the problem is considered quasi-static thermoelastic; while outside the thermal boundary layer, the temperature gradient is neglected and the problem is treated as an elastodynamic one with magnetic pressure on the cavity surface acting as an external force boundary condition.

BASIC EQUATIONS OF MAGNETO-THERMO-ELASTICITY

Let (r, θ, z) be cylindrical polar coordinates with the z-axis on the axis of cylindrical hole (Fig. 1). The region under consideration is a linear thermoelastic, electrically conducting medium in which there is no magnetic or electric polarization. Thus we consider only nonferromagnetic metals such as copper or aluminum. In the circular cavity a device exists which generates a time-dependent, axial magnetic field parallel to the axis of the cavity (Fig. 2) which we assume is known at the cavity surface $r = a$ for $t > 0$. In our further considerations we shall assume that the magnetic induction vector is reduced to the component $\boldsymbol{B} = (0, 0, B(r, t))$ acting along the direction of z-axis. Since the magnetic induction $\boldsymbol{B}$ is assumed to

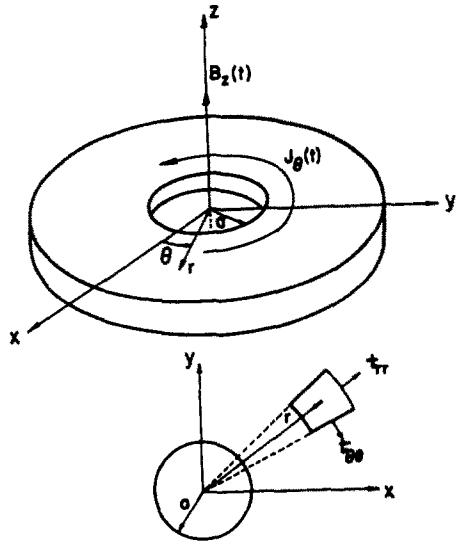

GEOMETRY OF LOADING

Fig. 1. Geometry of conducting solid, magnetic field and current.

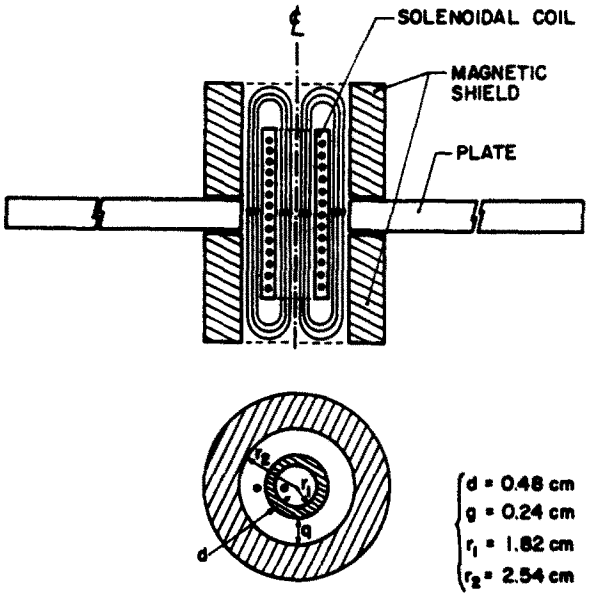

Fig. 2. Cross section of exciter coil and plate showing the magnetic flux in the coil-plate gap.

be constant along the z-axis, we shall consider bodies with cylindrical symmetry, with all quantities depending on the radial coordinate r and time t only. The electric field for $r > a$ is given by $\boldsymbol{E} = (0, E(r, t), 0)$.

The governing equations of momentum, energy, and electromagnetics in cylindrical coordinates are listed below, together with the concomitant constitutive relations:

$$\frac{\partial t_{rr}}{\partial r} + \frac{t_{rr} - t_{\theta\theta}}{r} + f_r = \rho \frac{\partial^2 u}{\partial t^2}$$

$$\rho c_v \frac{\partial T}{\partial t} + T_0 \beta \frac{\partial}{\partial t}\left(\frac{1}{r}\frac{\partial (ru)}{\partial r}\right) - \frac{\kappa}{r}\frac{\partial}{\partial r}\left(r \frac{\partial T}{\partial r}\right) = h$$

$$\frac{1}{r}\frac{\partial}{\partial r}(rE) + \frac{\partial B}{\partial t} = 0$$

$$-\frac{\partial B}{\partial r} = \mu_0 J$$

$$t_{rr} = (\lambda + 2\mu)\frac{\partial u}{\partial r} + \lambda \frac{u}{r} - \beta T$$

$$t_{\theta\theta} = (\lambda + 2\mu)\frac{u}{r} + \lambda \frac{\partial u}{\partial r} - \beta T$$

$$J = J' = \sigma E' = \sigma\left(E - B\frac{\partial u}{\partial t}\right)$$

where $\beta = \alpha(3\lambda + 2\mu)$.

The symbols used represent the following: initial and incremental temperature, T_0, T; specific heat at constant volume, c_v; coefficient of thermal conductivity, κ; thermal expansion coefficient, α; magnetic permeability, μ_0; electrical conductivity, σ; electric current density, J; elastic constants of Lamé, λ, μ; mass density, ρ; radial displacement, u; radial and circumferential stress, $t_{rr}, t_{\theta\theta}$. The displacement current in Maxwell's equations has been neglected. All constants are assumed to be independent of temperature.

The primes on J, E indicate field measured relative to a frame moving with the material point in which $J' = \sigma E'$ is assumed valid. Omission of the displacement current and free charges results in $J' = J$ [7].

With no magnetic or electric polarization, the component of the body force in the radial direction is given by the Lorentz body force

$$f_r = (J \times B) \cdot \hat{e}_r = JB$$

where $J = (0, J, 0)$. (For a discussion of magnetically induced stress waves in ferromagnetic conductors see Moon[13].)

The heat input per unit volume is given by Joule heating,

$$h = J' \cdot E' = \frac{J^2}{\sigma}.$$

The resulting set of equations coupling u, B, T becomes:

$$(\lambda + 2\mu)\left\{\frac{\partial}{\partial r}\left(\frac{1}{r}\frac{\partial (ru)}{\partial r}\right)\right\} - \rho \frac{\partial^2 u}{\partial t^2} = \frac{1}{2\mu_0}\frac{\partial B^2}{\partial r} + \beta \frac{\partial T}{\partial r} \tag{1}$$

$$\frac{\kappa}{r}\frac{\partial}{\partial r}\left(r\frac{\partial T}{\partial r}\right) - \rho c_v \frac{\partial T}{\partial t} = T_0 \beta \frac{\partial}{\partial t}\left(\frac{1}{r}\frac{\partial (ru)}{\partial r}\right) - \frac{1}{\sigma \mu_0^2}\left(\frac{\partial B}{\partial r}\right)^2 \tag{2}$$

$$\frac{1}{r}\frac{\partial}{\partial r}\left(r\frac{\partial B}{\partial r}\right) = \sigma\mu_0 \frac{\partial B}{\partial t} + \sigma\mu_0 \frac{1}{r}\frac{\partial}{\partial r}\left(rB\frac{\partial u}{\partial t}\right). \tag{3}$$

To simplify this set of coupled equations, we will drop the nonlinear term in Maxwell's equation for the magnetic field (3). This simplification is justified if one compares the two sources of the electrical field $\partial B/\partial t$ and $(1/r)(\partial/\partial r)(rB(\partial u/\partial t))$[3]. If one considers changes in magnetic field and stress in a time t_0, and distance δ; then the electric field is generated by terms whose estimates are given by

$$\frac{\partial B}{\partial t} : \frac{B_0}{t_0}$$

$$\frac{1}{r}\frac{\partial}{\partial r}\left(rB\frac{\partial u}{\partial t}\right) \begin{cases} \dfrac{1}{r}B\dfrac{\partial u}{\partial t} : \dfrac{B_0}{t_0}\dfrac{U_0}{\delta} \\ \dfrac{\partial B}{\partial r}\dfrac{\partial u}{\partial t} : \dfrac{B_0}{t_0}\dfrac{U_0}{\delta} \\ B\dfrac{\partial^2 u}{\partial r \partial t} = B\dfrac{\partial \epsilon_r}{\partial t} : \dfrac{B_0 t_{rr}}{(\lambda + 2\mu)t_0}. \end{cases}$$

Thus the convective term $(1/r)(\partial/\partial r)(rB(\partial u/\partial t))$ is negligible if $t_{rr}/\lambda + 2\mu$ and U_0/δ are small. As we shall see later the stress t_{rr} is bounded by $B_0^2/2\mu_0$, which for B_0 around 1 Weber/m^2, is of the order of 40 N/cm^2 (58 psi).

By integrating the stress we can obtain an estimate for the displacement at the surface at time t after the field is turned on,

$$U_0 \sim \frac{t_{rr}}{\lambda + 2\mu} c_p t$$

where c_p is the compressional wave speed. A good measure of the diffusion length of the magnetic field is

$$\delta \sim \left(\frac{\pi t}{\mu_0 \sigma}\right)^{1/2}.$$

Thus

$$\frac{U_0}{\delta} \sim \frac{B_0^2/2\mu_0}{\lambda + 2\mu} c_p \left(\frac{\mu_0 \sigma t}{\pi}\right)^{1/2}.$$

For aluminum and for magnetic fields of the order of 1 Weber/m^2

$$\frac{U_0}{\delta} \sim 0.1 t^{1/2}$$

where t is in seconds.

In high transient magnetic field devices the pulse time is usually less than 10^{-3} sec. Thus, for times less than 10^{-2} sec, the convective term is less than 1 per cent of the $\partial B/\partial t$ term. It is in this context that we neglect the nonlinear term in (3).

Thus we assume that the magnetic field satisfies the diffusion equation

$$\frac{1}{r}\frac{\partial}{\partial r}\left(r\frac{\partial B}{\partial r}\right) = \sigma\mu_0\frac{\partial B}{\partial t}. \tag{4}$$

These assumptions render B independent of the motion and temperature. The magnetic field simply becomes a source term to the coupled thermoelastic equations (1) and (2).

The solution of the magnetic diffusion equation (4) is sought for an infinite medium with a cylindrical cavity of radius a. The medium is supposed to be undisturbed and at zero magnetic induction initially.

When an oscillatory magnetic field

$$B(r = a, t) = B_0 \sin \omega t$$

is applied on the surface of the cavity, the value of B in the region $(a < r < \infty)$ is given by

$$B(r, t) = B_0\left(\frac{a}{r}\right)^{1/2} e^{-(r-a)/\delta} \sin\left(\omega t - \frac{(r-a)}{\delta}\right) \tag{5}$$

where $\delta = (2/\omega\sigma\mu_0)^{1/2}$ is the magnetic skin depth. This solution will be used only in estimating surface temperature rise due to a quasi-static thermal field rather than solve the transient problem.

A further simplification is made by writing the solution as the sum of three deformations as in[3], $u = u_B + u_T + u_c$, and two temperature fields $T = T_1 + T_2$. The equations (1) and (2) separate into the following equations:

$$(\lambda + 2\mu)\frac{\partial}{\partial r}\left(\frac{1}{r}\frac{\partial(ru_B)}{\partial r}\right) - \rho\frac{\partial^2 u_B}{\partial t^2} = \frac{1}{2\mu_0}\frac{\partial B^2}{\partial r} \tag{6}$$

$$(\lambda + 2\mu)\frac{\partial}{\partial r}\left(\frac{1}{r}\frac{\partial(ru_T)}{\partial r}\right) - \rho\frac{\partial^2 u_T}{\partial t^2} = \beta\frac{\partial T_1}{\partial r} \tag{7}$$

$$\frac{\kappa}{r}\frac{\partial}{\partial r}\left(r\frac{\partial T_1}{\partial r}\right) - \rho c_v\frac{\partial T_1}{\partial t} = -\frac{1}{\sigma\mu_0^2}\left(\frac{\partial B}{\partial r}\right)^2 \tag{8}$$

$$(\lambda + 2\mu)\frac{\partial}{\partial r}\left(\frac{1}{r}\frac{\partial(ru_c)}{\partial r}\right) - \rho\frac{\partial^2 u_c}{\partial t^2} - \beta\frac{\partial T_2}{\partial r} = 0 \tag{9}$$

$$\frac{\kappa}{r}\frac{\partial}{\partial r}\left(r\frac{\partial T_2}{\partial r}\right) - \rho c_v\frac{\partial T_2}{\partial t} - T_0\beta\frac{\partial}{\partial t}\left(\frac{1}{r}\frac{\partial(ru_c)}{\partial r}\right) = T_0\beta\frac{\partial}{\partial t}\left(\frac{1}{r}\frac{\partial(ru_B)}{\partial r} + \frac{1}{r}\frac{\partial(ru_T)}{\partial r}\right). \tag{10}$$

The solution of eqn (6), u_B, is called the eddy current pressure wave. Equations (7) and (8) constitute an uncoupled thermoelastic system where T_1 is generated by Joule heating, and u_T is an uncoupled thermoelastic wave.

Equations (9) and (10) involving u_c, T_2 are corrections to the uncoupled problem. The eddy current pressure wave u_B, and uncoupled thermoelastic wave u_T, act as sources. The corrections, u_c, T_2, are assumed to be small for early times.

THE INDUCED TEMPERATURE FIELD

During a magnetic field pulse, the temperature of the solid conductor adjacent to the applied magnetic field is raised by Joule heating. The solution for the magnetic field becomes input for the determination of the temperature, T_1, which along with B determines the stress.

If the thermal gradient term in eqn (8) is dropped, we have,

$$c_v T(r,t) = \frac{1}{\sigma\mu_0^2}\int_0^t \left[\frac{\partial B}{\partial r}\right]^2 dt. \tag{11}$$

To estimate the temperature rise at the surface of the cavity, we consider the case of an oscillatory magnetic field applied tangentially to the surface of the cavity. The magnetic field distribution $B(r,t)$ in the region $(a<r<\infty)$ is given by (5). Consider the case where the radius a is much larger than the magnetic skin depth $\delta(a \gg \delta)$. In the limit as $\delta/a \to 0$, the temperature field induced as given by (12) is

$$T(r,t) \cong \frac{\omega B_0^2}{2c_v\mu_0} e^{-2(r-a)/\delta}\left[t - \frac{1}{2\omega}\cos\left(\frac{2(r-a)}{\delta} - 2\omega t\right) + \frac{1}{2\omega}\cos\frac{2(r-a)}{\delta}\right]. \tag{12}$$

The surface temperature rise resulting from a half-cycle pulse $(t = \pi/\omega)$ is then†

$$T\left(a, \frac{\pi}{\omega}\right) = \frac{\pi}{2c_v\mu_0} B_0^2. \tag{13}$$

Note that this is independent of the frequency ω. The specific heat per unit volume for aluminum and copper at 20°C are 2.53×10^6 J/m$^3\cdot$°C and 3.43×10^6 J/m$^3\cdot$°C, respectively. Equation (13) becomes

$$\begin{aligned} T\left(a, \frac{\pi}{\omega}\right) &= 0.50 B_0^2\ ^\circ\text{C}/(\text{Wb/m}^2)^2 \text{ for aluminum} \\ T\left(a, \frac{\pi}{\omega}\right) &= 0.35 B_0^2\ ^\circ\text{C}/(\text{Wb/m}^2)^2 \text{ for copper.} \end{aligned} \tag{14}$$

A magnetic pulse of 3 Weber/m^2 therefore causes a surface temperature rise of about 4.5°C for an aluminum conductor, and 3.2°C for a copper conductor.

QUASI-STATIC THERMAL STRESSES

To estimate thermal stresses due to Joule heating in a homogeneous circular plate with a central hole we consider the temperature at the end of a half cycle or $\omega t = \pi$

$$T = T(r) = T_s\, e^{-2(r-a)/\delta} \tag{15}$$

where $T_s = \pi B_0^2/2c_v\mu_0$. The deformations and stresses in the plate will be functions of the radius only. As discussed in the introduction we assume the magnetic field pulse has a finite rise time so that inertia effects are small[6]. The Joule heating produced by eddy currents is confined in some finite boundary layer adjacent to the circular cavity. Within this thermal boundary layer the problem is considered quasi-static thermoelastic.

The boundary conditions for a circular plate with a central hole, having an inner radius a and an outer radius b are

$$t_{rr}(a) = 0, \quad t_{rr}(b) = 0. \tag{16}$$

†We recognize that for the transient case this is not accurate. However we believe it will suffice for an estimate to compare with the body force generated stresses.

Quasi-static thermal stresses are found to be [8, 9].

$$t_{rr}(r) = -\frac{T_s E\alpha\delta\, e^{2a/\delta}}{2r^2}\left\{\left(\frac{r^2-a^2}{b^2-a^2}\right)\left(e^{-2b/\delta}\left(b+\frac{\delta}{2}\right)-e^{-2a/\delta}\left(a+\frac{\delta}{2}\right)\right)\right.$$
$$\left.-\left(e^{-2r/\delta}\left(r+\frac{\delta}{2}\right)-e^{-2a/\delta}\left(a+\frac{\delta}{2}\right)\right)\right\} \tag{17}$$

and

$$t_{\theta\theta}(r) = -\frac{T_s E\alpha\delta\, e^{2a/\delta}}{2r^2}\left\{\left(\frac{r^2+a^2}{b^2-a^2}\right)\left(e^{-2b/\delta}\left(b+\frac{\delta}{2}\right)-e^{-2a/\delta}\left(a+\frac{\delta}{2}\right)\right)\right.$$
$$\left.+\left(e^{-2r/\delta}\left(r+\frac{\delta}{2}\right)-e^{-2a/\delta}\left(a+\frac{\delta}{2}\right)\right)\right\} - T_s E\alpha\, e^{-2(r-a)/\delta}. \tag{18}$$

In the limiting case where $\delta/a \ll 1$ and $b/a \gg 1$, (17) and (18) can be simplified to

$$t_{rr}(r) = -\frac{T_s E\alpha\delta}{2r^2}(a - r\, e^{-2(r-a)/\delta}) \tag{19}$$

and

$$t_{\theta\theta}(r) = \frac{T_s E\alpha\delta}{2r^2}(a - r\, e^{-2(r-a)/\delta}) - T_s E\alpha\, e^{-2(r-a)/\delta}. \tag{20}$$

The state of thermal stress is shown in Fig. 3 as a function of the radial coordinate r.

MAGNETIC PRESSURE INDUCED STRESS WAVES

The equation of motion for the magnetic pressure induced stress wave or the eddy current pressure wave is given by (6). When a conductor is subjected to a transient magnetic field, the induced eddy currents are concentrated near the boundary surface of the conductor adjacent to the exciting magnetic field. When the skin depth δ is small, the magnetic forces $J \times B$ on the conductor can sometimes be replaced by an equivalent magnetic pressure of intensity [1],

$$P_m = \frac{B_t^2}{2\mu_0} \tag{21}$$

where B_t is the tangential component of the magnetic field to the conductor surface. An

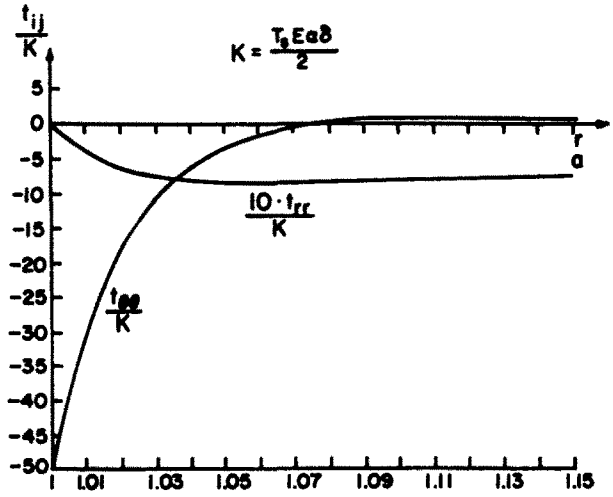

Fig. 3. Quasi-static thermal stresses at the end of a half cycle of magnetic pulse.

approximation can be made to reduce the body force problem to a surface force problem. The purpose of this approximation is only to determine the far field solution ($r \gg a$).

To justify this approximation, we consider a region with a circular cavity under the influence of a magnetic field applied axially in the cavity (Figs. 1 and 2). The equation of motion in cylindrical coordinates is

$$\frac{1}{r}\frac{\partial}{\partial r}(rt_{rr}) - \frac{t_{\theta\theta}}{r} + \frac{\partial P_m}{\partial r} = \rho\ddot{u}. \tag{22}$$

Integrating (22) over a region near the cavity:

$$\int_a^{a+\delta} \frac{\partial}{\partial r}(rt_{rr})\,dr - \int_a^{a+\delta} t_{\theta\theta}\,dr + \int_a^{a+\delta} r\frac{\partial P_m}{\partial r}\,dr = \int_a^{a+\delta} \rho r\ddot{u}\,dr. \tag{23}$$

Since $t_{rr}(a) = 0$, eqn (23) becomes,

$$(a+\delta)[t_{rr}(a+\delta) - P_m(a)] = \int_a^{a+\delta} (t_{\theta\theta} + P_m + \rho r\ddot{u})\,dr \tag{24}$$

or

$$(a+\delta)t_{rr}(a+\delta) - aP_m(a) \leq \delta|t_{\theta\theta} + P_m + \rho r\ddot{u}|_{\max}. \tag{25}$$

For fixed $|P_m|_{\max}$, the stored energy in the region tends to zero when $\delta/a \to 0$. This energy consideration can be expressed by

$$\lim_{\delta/a\to 0} \int_a^{a+\delta} (t_{\theta\theta}\epsilon_{\theta\theta} + t_{rr}\epsilon_{rr} + \rho\dot{u}^2)r\,dr \to 0. \tag{26}$$

Thus as $\frac{\delta}{a} \to 0$, $|t_{\theta\theta}\epsilon_{\theta\theta} + t_{rr}\epsilon_{rr} + \rho\dot{u}^2|_{\max}$ (27)

remains bounded.

If $u(r, t)$ is continuous and differentiable, we infer from this that $|t_{\theta\theta} + \rho r\ddot{u}|_{\max}$ remains bounded as $\delta/a \to 0$, so that from (25) we have

$$t_{rr}(a+\delta) \cong P_m(a). \tag{28}$$

Therefore, to determine the far field solution ($r - a \gg \delta$) and for that purpose alone, we set

$$t_{rr}(a, t) = P_m(t). \tag{29}$$

A body force problem is then reduced to a surface force problem.

This argument is supported by the work of Moon and Chattopadhyay[3] where the problem was solved as a 1-D inhomogeneous wave equation for a step magnetic field. They integrated the equation of motion using the method of characteristics. The stress at a distance equal to the skin depth was found to be equal to the magnetic pressure.

We consider therefore a region subjected to some uniform pressure $P_m(t)$, varying with time, at the boundary $r = a$ of the small hole at the center of the region (Fig. 1). The displacement equation of motion is

$$\frac{\partial^2 u}{\partial r^2} + \frac{1}{r}\frac{\partial u}{\partial r} - \frac{u}{r^2} = \frac{1}{c_p^2}\frac{\partial^2 u}{\partial t^2}, \quad r > a \tag{30}$$

where

$$c_p^2 = \frac{\lambda + 2\mu}{\rho}.$$

The solution for a step-function loading has been outlined by Kromm[10]. His solution involves the use of the Laplace transform technique.

The transient response $T_g(t)$ of an elastic body due to an arbitrary loading $g(t)$ can be determined by finding the response $T_h(t)$ due to a unit step-function loading $h(t)$ using the convolution integral:

$$T_g(t) = \int_0^t g'(\xi) T_h(t-\xi)\,d\xi \tag{31}$$

where $g(t) = 0$ for $t = 0$ is assumed. In this paper $g(t)$ is taken to be the magnetic pressure:

$$g(t) = P_m(t) = \frac{B_0^2}{2\mu_0}(e^{-\alpha t}\sin \Omega t)^2 = P_{m_0}(e^{-\alpha t}\sin \Omega t)^2, \quad t \geq 0. \tag{32}$$

Using a potential for the radial displacement, i.e. $u_r = \partial\phi/\partial r$, the radial and circumferential components of stress $t_{rr}, t_{\theta\theta}$ are related to the displacement potential ϕ by

$$t_{rr} = (\lambda + 2\mu)\nabla^2\phi - \frac{2\mu}{r}\frac{\partial\phi}{\partial r} \tag{33}$$

$$t_{\theta\theta} = (\lambda + 2\mu)\nabla^2\phi - 2\mu\frac{\partial^2\phi}{\partial r^2} \tag{34}$$

where ϕ satisfies the scalar wave equation with dilatational wave speed c_p. The boundary conditions are

$$t_{rr}(a, t) = -P_m(t), \quad \text{at } r = a \tag{35}$$

$$t_{rr} \to 0, \quad \text{as } r \to \infty. \tag{36}$$

A Fourier transform method has been used for scattering of a cylindrical object by Pao and Mow[11].

To solve the problem we employ the Fourier transform technique with respect to the time variable. In what follows, the radius and time are normalized, i.e. $r \equiv r/a$, $t \equiv c_p t/a$.

The solution for $\phi(r, t)$ satisfying boundary conditions (35) and (36) can be written in terms of the Hankel function of the first kind $H_0^{(1)}(\omega r)$[11].

$$\phi(r, t) = \frac{1}{2\pi}\int_{-\infty}^{\infty}\frac{\bar{P}_m(\omega)H_0^{(1)}(\omega r)}{F(\omega)}e^{-i\omega t}\frac{d\omega}{\omega} \tag{37}$$

where

$$F(\omega) = (\omega H_0^{(1)}(\omega) - 2\gamma H_1^{(1)}(\omega))(\lambda + 2\mu)/a^2; \ [\gamma = \mu/(\lambda + 2\mu)]$$

Numerical evaluation of (37) and the resulting stresses $t_{rr}, t_{\theta\theta}$ was done by first finding the zeros of $F(\omega)$ so the residues were determined. Second, a branch integral was numerically integrated.

Shown in Fig. 4 are the locations of the roots of $F(\omega)$ in a complex plane for $\nu = 0.3$. The two zeros of $F(\omega)$ were found to be $\pm 0.4226 - i0.3843$. The integral along $\int_{-\infty}^{\infty}$ is replaced by an appropriate contour integral. The selection of an appropriate contour c (Fig. 4) is dictated by the singularities of the integrand. The singularities in this case are a simple pole at the origin, a branch point at the origin due to the logarithmic singularity in the Hankel function, and simple poles at the zeros of $F(\omega)$ which is the denominator of the integrand.

Using the theorem of residues we finally obtain an expression for the circumferential stress

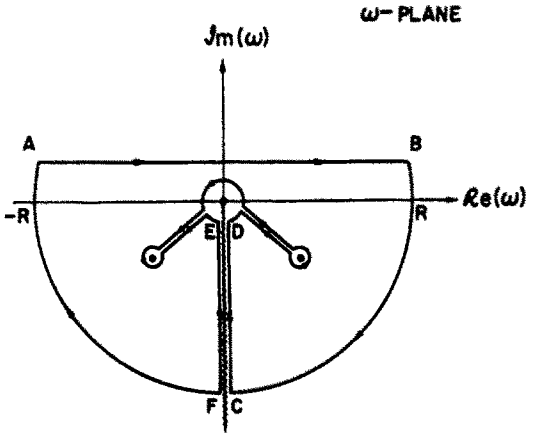

Fig. 4. Locations of zeros of $F(\omega)$ and path of integration.

due to a step-function loading which is useful for numerical computation:

$$\frac{t_{\theta\theta}(r,t)}{P_{m_0}} = \frac{1}{r^2} + \sum_{k=1}^{2}\left(\frac{1}{r}\cdot\frac{a_1 r\omega H_0^{(1)}(\omega r) - a_2 H_1^{(1)}(\omega r)}{(2-a_2)\omega H_0^{(1)}(\omega) - \omega^2 H_1^{(1)}(\omega)}\cdot e^{-i\omega t}\right)_{\omega=\omega_k} + \frac{1}{r}\int_0^\infty \frac{a_2(a_1 r-1)(I_1(\xi r)K_0(\xi r) + I_0(\xi r)K_1(\xi r))}{\pi^2(\xi I_0(\xi) - a_2 I_1(\xi))^2 + (\xi K_0(\xi) + a_2 K_1(\xi))^2} e^{-\xi t}\, d\xi \tag{38}$$

where $a_1 = 2\gamma - 1$, $a_2 = 2\gamma$ and I_n, K_n are modified Bessel functions of first and second kind, respectively. Similarly, for radial stress:

$$\frac{t_{rr}(r,t)}{P_{m_0}} = -\frac{1}{r^2} - \sum_{k=1}^{2}\left(\frac{1}{r}\cdot\frac{r\omega H_0^{(1)}(\omega r) - a_2 H_1^{(1)}(\omega r)}{(2-a_2)\omega H_0^{(1)}(\omega) - \omega^2 H_1^{(1)}(\omega)}\cdot e^{-i\omega t}\right)_{\omega=\omega_k} - \frac{1}{r}\int_0^\infty \frac{a_2(r-1)(I_1(\xi r)K_0(\xi r) + I_0(\xi r)K_1(\xi r)}{\pi^2(\xi I_0(\xi) - a_2 I_1(\xi))^2 + (\xi K_0(\xi) + a_2 K_1(\xi))^2} e^{-\xi t}\, d\xi \tag{39}$$

circumferential strain:

$$(\lambda+2\mu)\frac{\epsilon_\theta(r,t)}{P_{m_0}} = \frac{1}{a_2 r^2} + \frac{1}{r}\sum_{k=1}^{2}\left(\frac{-H_1^{(1)}(\omega r)}{(2-a_2)\omega H_0^{(1)}(\omega) - \omega^2 H_1^{(1)}(\omega)}\cdot e^{-i\omega t}\right)_{\omega=\omega_k} + \frac{1}{r}\int_0^\infty \frac{1}{\xi}\cdot\frac{I_1(\xi r)(\xi K_0(\xi) + a_2 K_1(\xi)) + K_1(\xi r)(\xi I_0(\xi) - a_2 I_1(\xi))}{(\xi K_0(\xi) + a_2 K_1(\xi))^2 + \pi^2(\xi I_0(\xi) - a_2 I_1(\xi))^2} e^{-\xi t}\, d\xi \tag{40}$$

radial strain:

$$(\lambda+2\mu)\frac{\epsilon_r(r,t)}{P_{m_0}} = -\frac{1}{a_2 r^2} + \frac{1}{r}\sum_{k=1}^{2}\left(\frac{H_1^{(1)}(\omega r) - \omega r H_0^{(1)}(\omega r)}{(2-a_2)\omega H_0^{(1)}(\omega) - \omega^2 H_1^{(1)}(\omega)}\cdot e^{-i\omega t}\right)_{\omega=\omega_k} + \frac{1}{r}\int_0^\infty \frac{1}{\xi}\cdot\frac{[\xi K_0(\xi) + a_2 K_1(\xi)][\xi I_0(\xi r) - I_1(\xi r)] - [\xi I_0(\xi) - a_2 I_1(\xi)][\xi r K_0(\xi r) + r K_1(\xi r)]}{[\xi K_0(\xi) + a_2 K_1(\xi)]^2 + \pi^2[\xi I_0(\xi) - a_2 I_1(\xi)]^2} \tag{41}$$

Numerical results of the transient response due to the magnetic pressure $P_m(t)$ of the form (32) were obtained for ϵ_θ and ϵ_r and then used to compare with the experimental data. The numerical program for calculating the stresses and strains due to a step loading was a modification of one developed by Dr. A. N. Cerangolu at Cornell University, Ithaca, N.Y. A listing of this program may be found in [12].

DESCRIPTION OF EXPERIMENT

The object of this experimental study, was to look at magnetically induced cylindrical stress waves in a large conducting plate. The goal was to compare the relative effects of the magnetic pressure and thermoelastic stresses. It will be shown that far field strains are due to magnetic pressure induced stress waves only. Thermal effects are confined to the skin depth for pulse times used in the experiment. The basic electrical circuit used in magnetic generation of stress waves is shown diagrammatically in Fig. 5. An axial magnetic field was generated by discharging stored charge in a capacitor bank through a solenoidal coil (Fig. 2). The conducting plate was placed symmetrically outside the coil. During the discharge, extremely high currents in the coil and plate produced a high magnetic field in the small air gap between the two. For example a bank voltage of 4 kV produced a current in the 9 turn coil of 51.6 kAmp. This current in turn produced a magnetic field at the surface of the plate of 3.8 Wb/m^2 or a magnetic pressure of 578 N/cm^2 (838 psi). The transient disturbances due to the interaction between the pulsed magnetic field and the induced eddy currents resulted in the propagation of stress waves in the conducting plate.

The maximum energy stored in the 360 μF capacitor bank was estimated at 4.5 kJ for a capacitor voltage of 5.0 kV.

A solenoidal coil was constructed to produce an axial magnetic field. An annealed beryllium copper rod of 4.8 mm (3/16 in.) diameter was wound onto a grooved Nylon mandrel. The diameter of the mandrel cross section is 4.6 cm. The pitch was at one turn per 1 cm.

A circular aluminum plate of 1.22 m (48 in.) diameter, 0.64 cm (1/4 in.) thickness was used as the specimen plate. A circular cavity of 2.54 cm (1 in.) radius was bored in the center of the plate. In order to produce a high magnetic pressure on the cavity surface two aluminum tubes of 2.54 cm (1 in.) inner radius, 0.64 (1/4 in.) thickness and 7 cm (2.75 in.) long were used as magnetic field shields (see Fig. 2). These shields were placed symmetrically outside the coil.

The current in the coil was measured by a small toroidal coil around the current lead, called a Rogowski coil. This coil produces a voltage proportional to the rate of change of current in the wire and when integrated gives the current directly. The magnetic field at the cavity surface was measured by using a small search coil of 50 turns and 1.8 mm in diameter. The rate of change of magnetic flux in the coil produces a measurable voltage.

The strain in the specimen plate was measured by semiconductor resistance strain gates at a radius of 29.2 cm (11.5 in.). Two gages were placed symmetrically opposed on each surface. The outputs from the two gages were then added in a Wheatstone bridge to cancel any bending disturbance in the plate. The strain output as well as the integrated Rogowski coil voltage were recorded on a storage oscilloscope as shown in Fig. 6.

Chromel–constantan thermocouples were employed to measure the temperature rise in the plate near the hole during the capacitor bank discharge. The dimensions of the thermocouple wires were 0.0013 in. diameter with approx. 0.0039 cm diameter beads. The response time of the thermocouple is 0.003 sec. The thermocouples were mounted in minute holes drilled in a long hollow aluminum cylinder at predetermined locations.

The resulting pulse current shapes were heavily damped sine waves (Fig. 6, top trace), with a pulse length of about 67 μsec and a rise time of about 26 μsec. This produced a compressional stress pulse about 36 cm long in the aluminum plate.

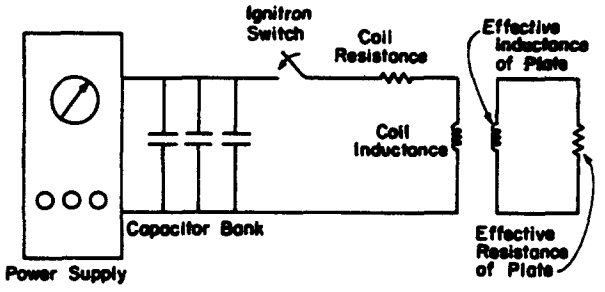

Fig. 5. Schematic of magnetic field generator.

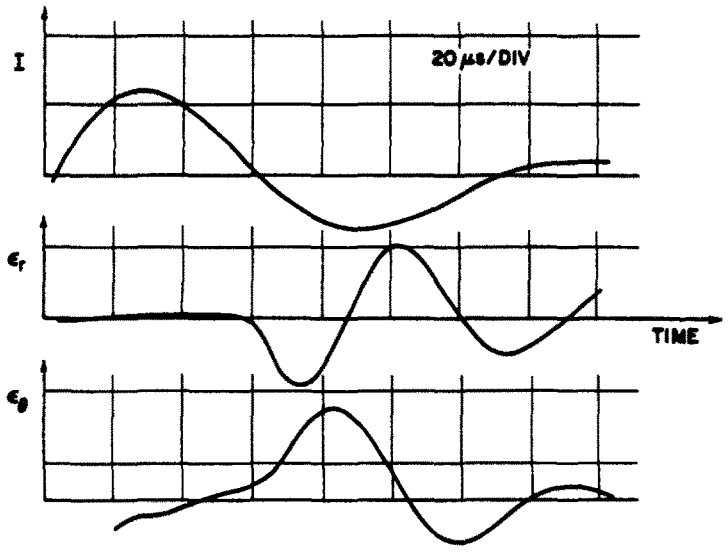

Fig. 6. I, ϵ_r, and ϵ_θ vs time (at 4 kV).

COMPARISON OF THEORY AND EXPERIMENT

The theoretical calculations in eqns (40)–(41) were based on the assumption of *plane strain* while experiments on the aluminum plate are under conditions of *plane stress*. In order to compare these two results, the experimental strain measurements were multiplied by $(1-\nu^2)$ where ν is Poisson's ratio.

The experimental data confirm the theoretical prediction that the strains and temperature generated in the specimen plate are proportional to B^2 as shown in Fig. 7. Experimental measurements of the dynamic magnetically induced strains show very good agreement with the computed analytical solution using the surface magnetic pressure approximation (Fig. 8). Therefore, we conclude that the dynamic thermoelastic wave is negligible. It is sufficient to assume the quasi-static thermoelastic state near the circular cavity.

The difference between measured and theoretically produced stress waves is within 10% in most of the cases (Fig. 8). The numerical calculations were obtained for the peak stress values

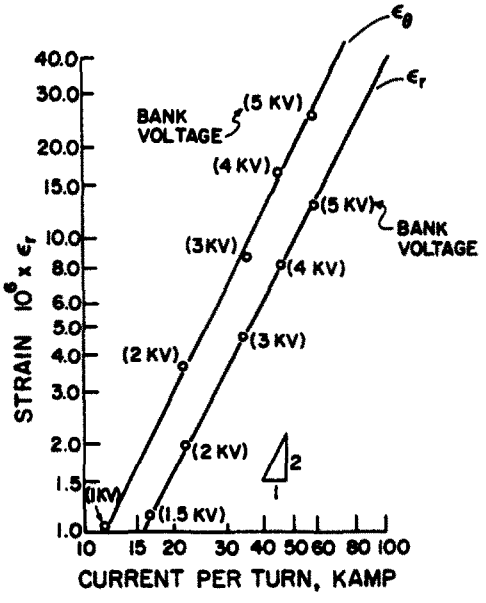

Fig. 7. Experimental radial and circumferential strain vs current (log–log scale).

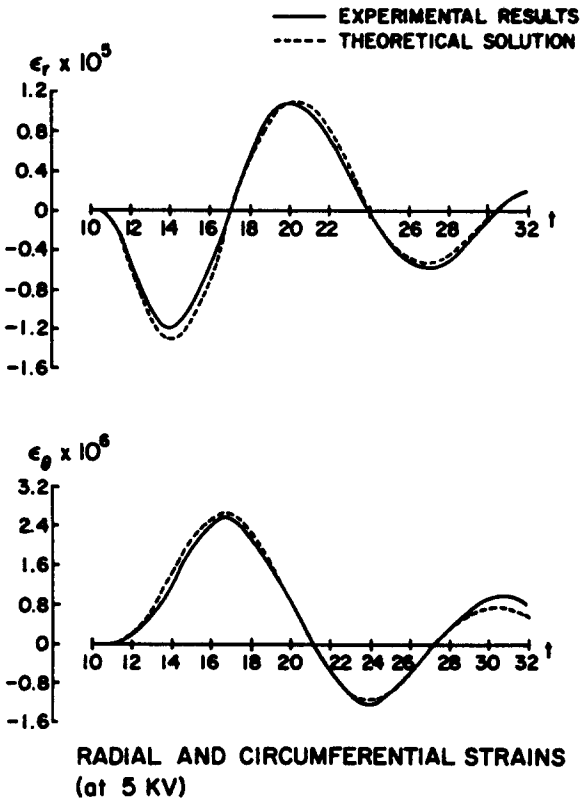

Fig. 8. Circumferential strain vs time (top).
Radial strain vs time (bottom) at 5 kV.

for $r/a = 1$ (cavity) and $r/a = 11.5$ (strain gage). It was found that the peak $t_{\theta\theta}$ at the strain gage location is about 5% of the peak $t_{\theta\theta}$ at the cavity (Fig. 9).

The quasi-static temperature distribution in the thermal boundary layer has a maximum value on the cavity surface, which is proportional to the Joule heating or square of the current as shown in Fig. 10. The measured induced temperature vs radius compares well with the theoretical value using a harmonic magnetic field (Fig. 11). This temperature rise produces a peak compressive circumferential thermal stress near the cavity. When the current pulse

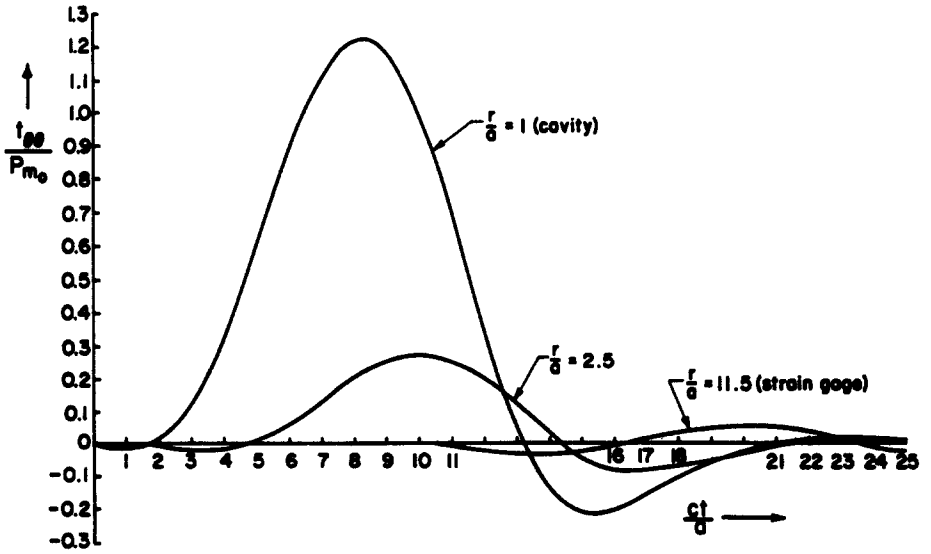

Fig. 9. Eddy current induced stress wave vs non-dimensionalized time.

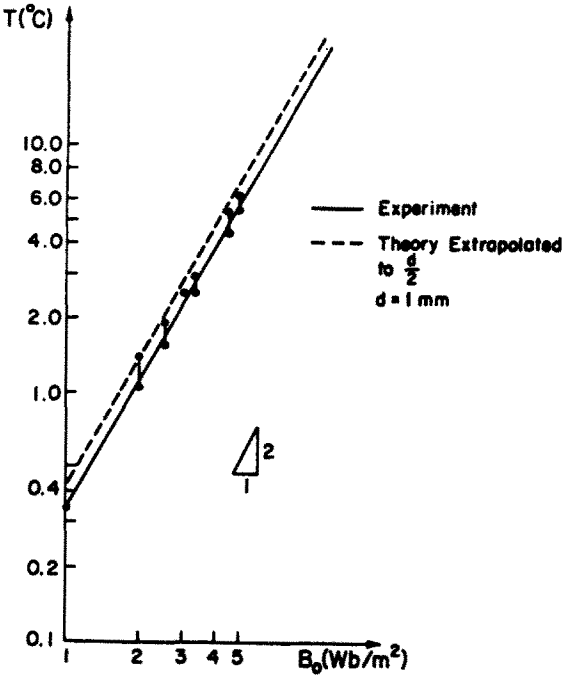

TEMPERATURE RISE AT $\frac{d}{2}$ vs B_0

Fig. 10. Induced temperature vs magnetic field (log-log scale).

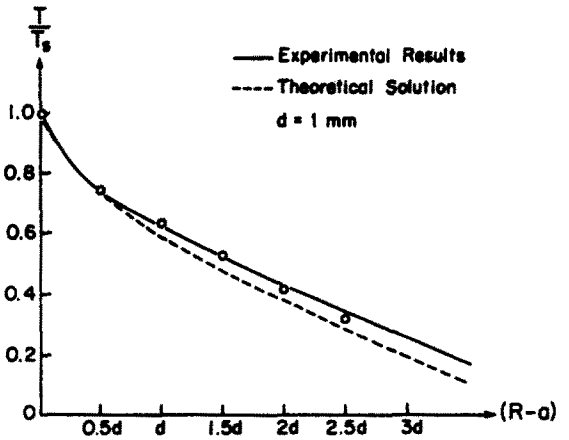

TEMPERATURE DISTRIBUTION NEAR THE CAVITY

Fig. 11. Induced temperature distribution vs radius.

duration is very small, the peak thermal stress can reach as much as three times the maximum dynamically induced stress. A comparison of the quasi-static thermal stress near the cavity and the eddy current induced stress wave is shown in Fig. 12.

CONCLUSIONS

Both the analytical and experimental results of this study confirm the fact that, for magnetic fields of rise times of the order of 20 μsec or greater, the induced thermoelastic wave due to Joule heating is negligible. However this study does show that quasi steady thermal stresses due

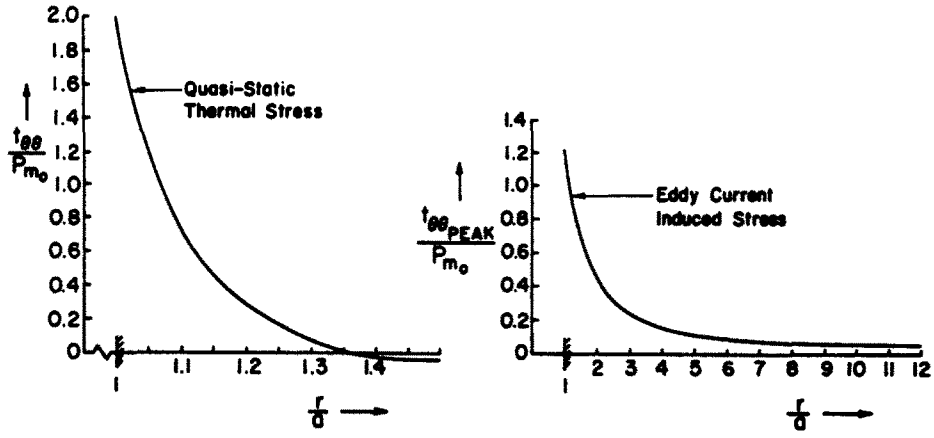

Fig. 12. Comparison of quasi-static thermal stress and eddy current induced stress wave.

to Joule heating can produce stresses in the conductor, near the source of the magnetic field, greater than those generated by the Lorentz body forces. These results suggest that quasi steady thermoelastic stresses should be considered in the analysis of magnetic forming processes.

Finally the excellent agreement between analytical calculations and measurements of dynamic stress waves in the far field confirms the validity of the "magnetic pressure" approximation in replacing a body force problem by a surface traction problem.

REFERENCES

1. H. P. Furth, Magnetic pressure. *Int. Sci. Tech.* 32 (1966).
2. L. W. Morland, Generation of thermoelastic stress waves by impulsive electromagnetic radiation. *AIAA J.* 6(6), 1063 (1968).
3. F. C. Moon and S. Chattopadhyay, Magnetically induced stress waves in a conducting solid–theory and experiment. *J. Appl. Mech.* 41(3), *Trans. ASME* 96, Series E 641 (1974).
4. V. I. Danilovskaya, Thermal stress in an elastic half-space arising after a sudden heating of its boundary (in Russian). *Prikladnaya Matematika i Mechanika* 14, 316–318 (1950).
5. B. A. Boley and I. S. Tolins, Transient coupled thermoelastic boundary value problems in the half space. *J. Appl. Mech.* 637–646 (1962).
6. E. Sternberg and J. G. Chakravorty, On inertia effects in a transient thermoelastic problem. *J. Appl. Mech.* 26, *Trans. ASME* 81, Series E 503 (1959).
7. A. Sommerfeld, *Electrodynamics*, p. 280. Academic Press, New York (1964).
8. B. A. Boley and J. H. Weiner, *Theory of Thermal Stresses*. Wiley, New York (1960).
9. W. Nowacki, *Thermoelasticity*. Addison-Wesley, Reading, Mass. 1962.
10. A. Kromm, On the propagation of stress waves in circular cylindrical plates (In German). *Zeit. Angew. Math. Mech.* 28(4), 104–114, 297–303 (1948).
11. Y. H. Pao and C. C. Mow, *Diffraction of Elastic Waves and Dynamic Stress Concentration*. Crane Russak Publ. (1971).
12. C. T. Chian, Magnetically induced cylindrical stress waves in a thermoelastic conductor, Doctoral dissertation, Cornell University (May 1978).
13. F. C. Moon, Problems in magneto-solid mechanics. *Mechanics Today* (Edited by S. Nemat-Nasser), Vol. 4. Pergamon Press, Oxford (1978).